Articles

Structural Characterization of a 140° Domain Movement in the Two-Step Reaction Catalyzed by 4-Chlorobenzoate:CoA Ligase[†,‡]

Albert S. Reger,[§] Rui Wu,[⊥] Debra Dunaway-Mariano,[⊥] and Andrew M. Gulick*[,§]

Hauptman-Woodward Medical Research Institute, Buffalo, New York 14203 and Department of Structural Biology, State University of New York at Buffalo, Buffalo, New York 14203, and the Department of Chemistry and Chemical Biology, University of New Mexico, Albuquerque, New Mexico 87131

Received April 21, 2008; Revised Manuscript Received June 4, 2008

ABSTRACT: Members of the adenylate-forming family of enzymes play a role in the metabolism of halogenated aromatics and of short, medium, and long chain fatty acids, as well as in the biosynthesis of menaquinone, peptide antibiotics, and peptide siderophores. This family includes a subfamily of acyl- and aryl-CoA ligases that catalyze thioester synthesis through two half-reactions. A carboxylate substrate first reacts with ATP to form an acyl-adenylate. Subsequent to the release of the product PP_i, the enzyme binds CoA, which attacks the activated acyl group to displace AMP. Structural and functional studies on different family members suggest that these enzymes alternate between two conformations during catalysis of the two half-reactions. Specifically, after the initial adenylation step, the C-terminal domain rotates by ~140° to adopt a second conformation for thioester formation. Previously, we determined the structure of 4-chlorobenzoate:CoA ligase (CBL) in the adenylate forming conformation bound to 4-chlorobenzoate. We have determined two new crystal structures. We have determined the structure of CBL in the original adenylate-forming conformation, bound to the adenylate intermediate. Additionally, we have used a novel product analogue, 4-chlorophenacyl-CoA, to trap the enzyme in the thioester-forming conformation and determined this structure in a new crystal form. This work identifies a novel binding pocket for the CoA nucleotide. The structures presented herein provide the foundation for biochemical analyses presented in the accompanying manuscript in this issue [Wu et al. (2008) *Biochemistry 47*, 8026−8039]. The complete characterization of this enzyme allows us to provide an explanation for the use of the domain alternation strategy by these enzymes.

Enzymes are known to use conformational changes as an important component of their catalytic mechanism. The increasing number of protein structures, coupled with functional studies and molecular dynamics simulations, have provided a more complete awareness of the range of motions that can take place. These structural changes serve many functions, acting as selectivity filters by interacting with nonreacting groups on substrates (*1*), forming closed active sites to trap or desolvate reactive intermediates (*2*), or energetically straining substrates to promote the formation of transition state like complexes (*3*). Often, these protein movements are relatively small loop closures that allow an enzyme to adopt an "open" and a "closed" state, depending on the contents of the active site.

Potentially more interesting are larger domain movements that are known to occur in multidomain enzymes. These movements can result in rotations of greater than 50° and in net translation of protein groups or protein-bound intermediates by dozens of angstroms. Recent structures of large protein machines such as the fatty acid synthase (*4, 5*) and pyruvate carboxylase (*6*) demonstrate how these enzymes use pantetheine or biotin based cofactors to transport reactants to active sites located within different protein domains. Studies of pyruvate phosphate dikinase illustrate

[†] This work was supported by NIH Grant GM-68440 to A.M.G. and by NIH Grant NIH GM-36260 to D.D.-M. Use of the National Synchrotron Light Source, Brookhaven National Laboratory, was supported by the U.S. Department of Energy, Office of Science, Office of Basic Energy Sciences, under Contract No. DE-AC02-98CH10886. Additionally, portions of this research were carried out at the Stanford Synchrotron Radiation Laboratory, a national user facility operated by Stanford University on behalf of the U.S. Department of Energy, Office of Basic Energy Sciences. The SSRL Structural Molecular Biology Program is supported by the Department of Energy, Office of Biological and Environmental Research, and by the National Institutes of Health, National Center for Research Resources, Biomedical Technology Program, and the National Institute of General Medical Sciences.

[‡] The structure factors and coordinates for the 4-chlorobenzoate:CoA ligase bound to 4-chlorobenzoyladenylate-5′-phosphate have been deposited with the Protein Data Bank (3CW8). The structure factors and coordinates for the 4-chlorobenzoate:CoA ligase bound to 4-chlorophenacyl-CoA and AMP have been deposited with the Protein Data Bank (3CW9).

* To whom correspondence should be addressed. Tel.: (716) 898-8619. Fax: (716) 898-8660. E-mail: gulick@hwi.buffalo.edu.

[§] Hauptman-Woodward Medical Research Institute and State University of New York at Buffalo.

[⊥] University of New Mexico.

10.1021/bi800696y CCC: $40.75
Published on Web 07/12/2008

Table 1: Conserved Sequence Motifs within the PF00501 Adenylate-Forming Family of Enzymes

sequence[a]	Chang[b]	Marahiel[b]
Tyr^{160}-(Thr/Ser)-(Thr/Ser)-Gly-(Thr/Ser)-(Thr/Ser)-X-Pro-Lys	Motif I	A3
$(Asn^{302}$/Asp)-X-(Tyr/Trp/Phe)-Gly-X-Thr-Glu	Motif II	A5
(Phe/Tyr^{381})-X-(Ser/Thr)-Gly-Asp	Motif III	A7
Gly^{399}-Arg-X-(Lys/Asp)-Asp-X_5-Gly		A8
Pro^{486}-X_4-Gly-Lys		A10

[a] The residue position of the first residue of the sequence motif is indicated for CBL. [b] Nomenclature in column one has been adopted primarily for the aryl and acyl-CoA ligases (*14*), while those in the second column were adopted for the NRPS adenylation domains (*15*).

another large domain movement to transport a phosphoryl group, via a phosphohistidine residue, from a nucleotide binding domain to a second catalytic domain where the phosphate is transferred to the pyruvate substrate (*7*). The term *domain alternation* was used to describe a large conformational change in the B12-dependent methionine synthase (*8*). In this enzyme, a 90° domain rotation is used to transfer the inactive cob(II)alamin cofactor to an activation domain where it is reactivated by reductive methylation.

We have proposed a second type of large-scale domain rearrangement for a family of adenylate-forming enzymes that catalyze a two-step reaction that converts an organic acid to a CoA thioester (*9, 10*). In these adenylate-forming enzymes, *domain alternation* is used not to transport a substrate between active sites but to reconfigure a single active site for multiple catalytic steps.

The acyl- and aryl-CoA synthetases/ligases, the adenylation domains of non-ribosomal peptide synthetases (NRPSs),[1] and firefly luciferase enzymes constitute this adenylate-forming family (*11–13*). These enzymes (PFAM00501) are relatively large, with sizes ranging from 500 to 700 residues, and are composed of two structural domains, a larger N-terminal domain of 400−550 residues and a smaller C-terminal domain of 100−140 residues. Family members share limited sequence homology of ~20−30%. Nonetheless, several well-conserved sequence motifs exist between members; multiple names have been assigned by different investigators (*14, 15*) to these regions (Table 1).

In the reaction catalyzed by enzymes within this family, a substrate carboxylate is activated with ATP to form an acyl-adenylate. The second half-reactions are more diverse with the enzymes catalyzing thioester formation with either CoA or a pantetheine cofactor of an acyl-carrier protein, or catalyzing oxidative decarboxylation in the case of firefly luciferase.

A number of structures of members of the adenylate-forming enzyme family have been determined (*9, 10, 16–24*). These structures provide many insights into the acyl binding pocket, which has been explored through directed mutagenesis to alter substrate specificity in a number of enzymes in this family (*19, 25–27*).

The structures of adenylate-forming enzymes have revealed two strikingly different conformations. The C-terminal domain adopts one of two orientations that differ from each other by a 140° rotation around a hinge residue of the A8 motif. These structural studies, supported by biochemical analysis (*10, 28*), have suggested that enzymes within this family adopt one conformation to catalyze the adenylation half-reaction. The C-terminal domain then rotates to a distinct conformation used for the second half-reaction. Alternate faces of this C-terminal domain are therefore presented to a single active site for the different catalytic steps. The benefit derived from this catalytic strategy has not yet been identified.

We have previously determined the structures of 4-chlorobenzoate:CoA ligase (CBL) in the adenylate-forming conformation in both the unliganded and 4-CB-bound states. CBL catalyzes the two-step activation of 4-CB (Figure 1) to 4-CB-CoA in the degradation of this halogenated aromatic compound (*29*). We present here new structures of 4-chlorobenzoate:CoA ligase in both the adenylate- and thioester-forming conformations. The active site residues are compared to those identified in other family member structures and are further explored kinetically in the accompanying manuscript in this issue (*30*). Interestingly, the structure of CBL bound to 4-chlorophenacyl-CoA identifies a novel CoA binding pocket compared to the pocket identified in Acs (*9*). This combination of structural and functional investigation now explains the use of domain alternation by the adenylate-forming enzyme superfamily.

MATERIALS AND METHODS

Crystallization of CBL Bound to 4-Chlorobenzoyl-AMP. The His-tagged wild-type CBL was prepared as described previously and dialyzed into in 50 mM K^+HEPES (pH 7.5 at 25 °C) containing 1 mM DTT (*19*). Protein at 10 mg/mL was combined with ATP and 4-chlorobenzoate to a final concentration of 1 mM each. Crystals were grown by hanging-drop vapor diffusion at 4 °C using 16−24% pentaerythritol propoxylate 426 (*31*), and 0.1 M K^+HEPES (pH 6.5 or 6.75). Crystals were cryoprotected by transferring through six solutions containing increasing amounts of ethylene glycol for approximately 1 min each. The final cryoprotectant contained 24% pentaerythritol propoxylate 426, 24% ethylene glycol, and 0.1 M K^+HEPES and 1 mM ATP and 1 mM 4-chlorobenzoate.

Crystallographic Data Collection and Structure Refinement of the CBL(4-Chlorobenzoyl-AMP) Complex. Data for wild-type CBL were collected at the National Synchrotron Light Source at Brookhaven National Laboratory at beamline X4A. The structure was solved by molecular replacement using MOLREP (*32*) of the CCP4 package (*33*). The CBL(4-chlorobenzoate) structure (1T5H) with all nonprotein atoms removed was used as the search model. Refinement was performed with REFMAC5 (*34*). As the refinement neared completion, TLS anisotropic refinement (*35*) was included for the N- and C-terminal domains, as well as for the adenylate ligand, which resulted in a drop in the R-free value.

[1] Abbreviations used are 4-CB, 4-chlorobenzoate; CoA, coenzyme A; CBL, 4-chlorobenzoate: CoA ligase; 4-CB-AMP, 4-chlorobenzoyl-adenosine-5′-monophosphate; 4-CP-CoA, 4-chlorophenacyl-CoA, PP_i, inorganic pyrophosphate; ATP, adenosine-5′-triphosphate; AMP, adenosine-5′-monophosphate; AMPPNP, adenosine-5′-(β,γ-imido)triphosphate; NADH, β-nicotinamide adenine dinucleotide; PEP, phosphoenol pyruvate; DTT, dithiothreitol; K^+HEPES, potassium salt of *N*-(2-hydroxyethyl)piperzine-*N*′-2-ethanesulfonate; MOPS, 3-(*N*-morpholino)propane sulfonic acid; rms, root-mean-square; SDS−PAGE, sodium dodecylsulfate−polyacrylamide gel electrophoresis; PheA, the phenylalanine-activing domain of GrsA; NRPS, nonribosomal peptide synthetase; DVR/T, drop-volume ratio and temperature method of crystallization optimization.

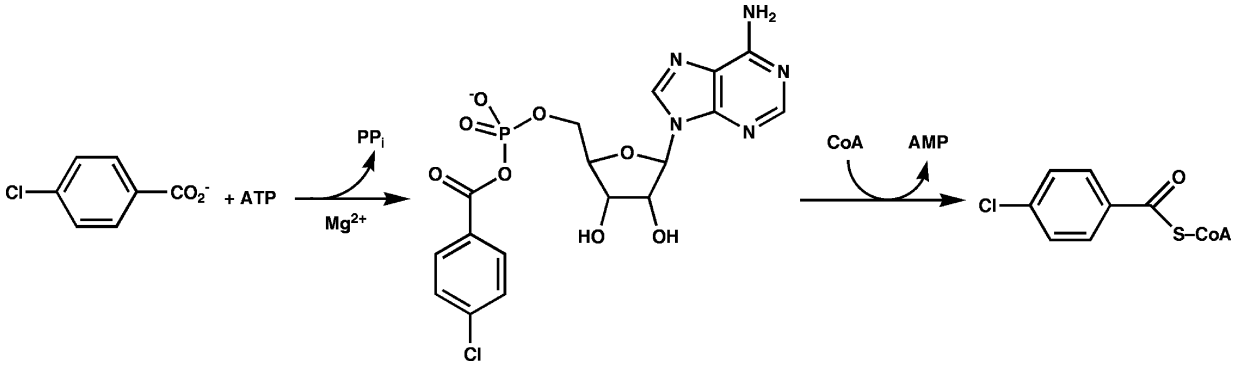

FIGURE 1: Two-step chemical reaction catalyzed by 4-chlorobenzoyl-CoA ligase.

Table 2: Crystallographic and Refinement Statistics for CBL Bound with 4-CB-AMP or Bound to 4-CP-CoA and AMP

	CBL + 4-CB-AMP	CBL + AMP and 4-CP-CoA
resolution	25−2.25 Å	35−2.0 Å
space group	$P3_221$	$P2_12_12_1$
unit cell	a = 128.6 Å	a = 60.5 Å
	b = 128.6 Å	b = 87.8 Å
	c = 72.3 Å	c = 186.1 Å
R_{merge}[a]	5.2% (48.0%)	8.6% (17.4%)
completeness[a]	97.7% (88.6%)	94.6% (74.3%)
I/σ[a]	18.4 (2.3)	30.9 (6.7)
# observations	161074	360210
# reflections	32168	64355
refinement resolution	15.0−2.25 Å	35.0−2.0 Å
R_{cryst} (overall/highest resolution shell)[a]	19.6% (25.7%)	16.6% (17.4%)
R_{free} (overall/highest resolution shell)[a]	25.7% (31.2%)	20.9% (26.4%)
Wilson B-factor	60.5 Å^2	18.9 Å^2
average B-factor, overall	57.7 Å^2	A = 18.8 Å^2, 19.3 Å^2
		B = 17.4 Å^2, 18.2 Å^2
average B-factor, protein (N-term)[b]	56.0 Å^2, 55.9 Å^2	A = 18.0 Å^2, 18.6 Å^2
		B = 16.8 Å^2, 17.5 Å^2
average B-Factor, protein (C-term)[b]	60.7 Å^2, 64.1 Å^2	A = 21.5 Å^2, 21.9 Å^2
		B = 19.9 Å^2, 20.8 Å^2
average B-Factor, solvent	57.1 Å^2	26.1 Å^2
rms deviation bond lengths, angles	0.015 Å, 1.45°	0.008 Å, 1.24°

[a] Values for the highest resolution shell (2.35−2.25 Å) are given in parentheses. [b] The two numbers refer to average B-factors for main chain and side chain atoms, respectively.

The electron density for the adenine base was unambiguous. Density was present for a molecule of 4-CB; however, the density was not as strong as in the earlier model nor as strong as the density for the adenine base. Contoured at 2.5σ, a small region of positive difference density was observed near the phosphate. Attempts to refine the model with a Mg^{2+} ion, or combinations of ATP, ADP, and 4-CB-AMP were unsatisfactory and we concluded that the 4-CB-AMP could best model the active site contents. The mean B-factor for the AMP portion of the ligand, calculated in the absence of TLS refinement, is 66 Å^2, slightly higher than that observed for all atoms. In contrast, the values for the 4-CB moiety are higher still, at 86 Å^2. Because the ligand was assigned as a TLS refinement group for anisotropic TLS refinement and because of the high overall Wilson B-value for this data set, we did not further adjust the occupancy of the ligand. Data collection and refinement statistics are presented in Table 2.

Crystallization and Structure Determination of the CBL(4-CP-CoA)(AMP). The inhibitor 4-chlorophenacyl CoA was synthesized as described (*30, 36*). To identify new crystallization conditions for the CBL enzyme bound to 4-chlorophenacyl-CoA, protein was screened using the High-Throughput Screening laboratory available at the Center for High Throughput Structural Biology, housed at Hauptman-Woodward Institute (*37*) and optimized using the DVR/T method (*38, 39*); both were performed using the batch method. Crystal production was subsequently scaled up and optimized via hanging drop vapor diffusion using 14−18% PEG 1000, 50−100 mM magnesium nitrate and 100 mM MOPS, pH 7.0. The ligands, AMP and 4-CP-CoA, were added at a concentation of 1 mM prior to crystallization. Cryoprotection was performed by soaking crystals for 1 min in a cryoprotectant of increasing ethylene glycol concentration. The final cryoprotectant solution contained 20% PEG 1000, 75 mM magnesium nitrate, 24% ethylene glycol, and 100 mM MOPS pH 7.0 and included 1 mM 4-chlorophenacyl-CoA and AMP.

Data collection for the new CBL structure was performed at Hauptman-Woodward Institute using remote access to the Stanford Synchrotron Radiation Laboratory (SSRL) (*40*). Data were collected remotely on beamline 9-1. Intensity data were processed with MOSFLM and SCALA (*41*). TRUNCATE of the CCP4 package (*33*) was used to convert the intensities to structure factors. The molecular replacement program MOLREP (*32*) of the CCP4 package was used for phasing. Only the N-terminal domain of CBL (residues 1−402) was used as a search model to limit model bias of the C-terminal domain orientation. Two molecules were identified in the asymmetric unit. Model refinement was

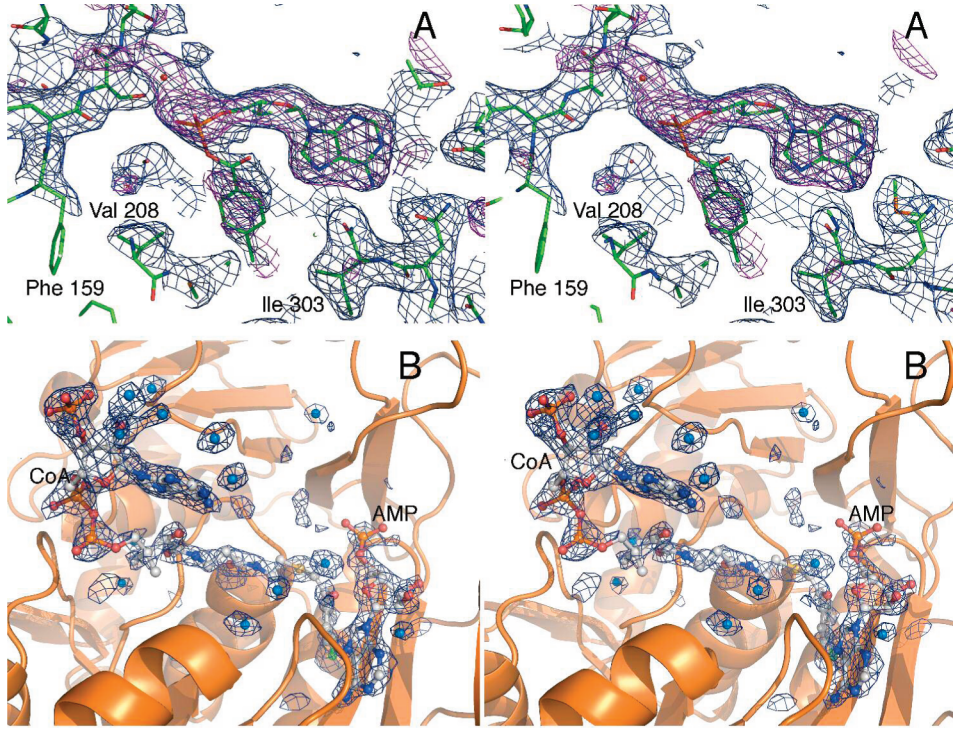

FIGURE 2: Electron density of the active site ligands in the two crystal structures. (A) Electron density of the adenylate formed in the active site of the CBL enzyme is shown in stereo representation. Density formed with coefficients of the form 2Fo-Fc, calculated at the end of refinement, is shown in blue contoured at 1σ. Also included in the figure in magenta is electron density calculated with coefficients of the form Fo-Fc, generated prior to the inclusion of the adenylate ligand into the refinement, and contoured at 2.5σ. The unbiased density illustrates that the AMP is better ordered than the 4-CB moiety. (B) Electron density of the 4-chlorophenacyl-CoA ligand and AMP bound to the CBL enzyme determined in the thioester-forming conformation. Density was calculated with Fo-Fc coefficients calculated prior to inclusion of either ligand in the molecular model and contoured at 3.5σ.

carried out by the program REFMAC5 (*34*), using weighted individual atomic B-factors. The program COOT was used to build the C-terminal domain de novo and to model the complete molecule (*42*). The find water option of COOT, confirmed with manual inspection, was used to place waters into spherical difference density greater than 2.5σ. TLS anisotropic refinement was performed on the N- and C-terminal domains at the completion of the model building process (*35*). An accompanying decrease in the R_{free} was observed. The final model is missing the last residue on both molecules in the asymmetric unit and residue 490 could not be modeled in chain A.

Additional Software. The crystallographic model was compared with prior structures for the analysis of domain orientation with the program DYNDOM (*43*). Figures were prepared with PYMOL (*44*).

RESULTS

Structure Determination of CBL Bound to the 4-Chlorobenzoyladenylate. Overall Structure. Crystals of the CBL enzyme bound to 4-CB-AMP were grown under conditions similar to those identified previously for the formation of CBL Ile303 mutants bound to chlorobenzoates (*19*). The final model for the wild-type CBL cocrystallized with ATP and 4-CB contains 501 residues, a molecule of 4-CB-AMP, and 135 water molecules. There is a short disordered segment in the model at residues 438−440 with no density present for Arg439. The final refinement statistics are presented in Table 2. The electron density map of the active site is shown in Figure 2. The data exhibit some degree of disorder, reflected by the high B-factors, however the model was conservatively refined and agrees well with prior structural information.

The CBL(4-CB-AMP) structure is composed of the large N-terminal domain and the smaller C-terminal domain, as observed previously for the unliganded CBL and CBL(4-CB) structures. The root-mean-square distance of Cα positions calculated between the CBL(4-CB-AMP) structure and the previous structures is ∼1 Å over the full length of the protein. In general, the structures superimpose well; however, two loops adopt alternate conformations. The loop composed of residues Ala263 to Lys270 is >20 Å from the active site and the alternate conformation does not appear to be a direct result of the presence of the 4-CB-AMP at the active site. In contrast, residues 280–282, as discussed below, adopt a new orientation to accommodate the bound nucleotide.

The 4-CB-AMP Binding Site. The active site is positioned at the interface of the two domains. The density observed in this region is consistent with a bound 4-CB-AMP ligand, although it is likely that alternate ligand combinations (ATP alone, AMP + 4-CB, most likely) are present in some molecules within the crystal lattice (Figure 2A). Thus, the 4-CB and ATP, which were included in the crystallization solution, underwent the catalyzed reaction in the absence of added Mg^{2+} cofactor. Studies of CBL activation by Mg^{2+} have shown that CBL retains a low level of catalytic activity in assay solutions that do not contain added Mg^{2+} (see the accompanying manuscript in this issue (*30*)). The protein residues that interact with the 4-CB-AMP ligand are shown in Figure 3. Many of these interactions are conserved throughout the adenylate-forming family. There is a hydrogen

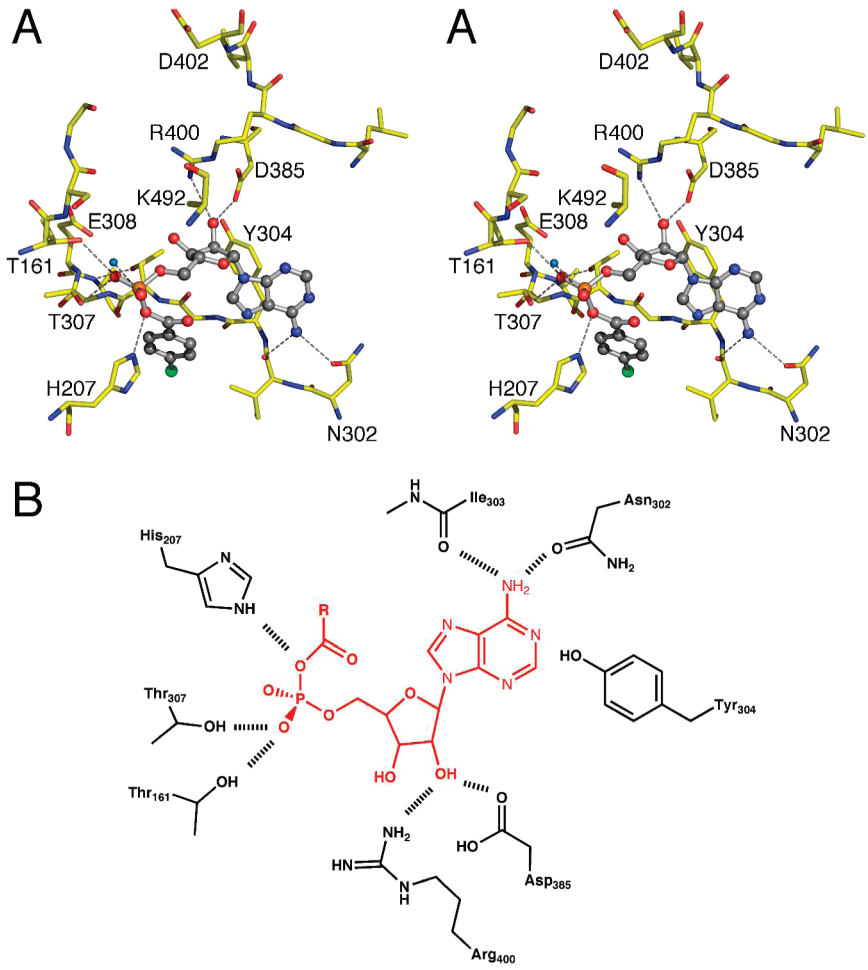

FIGURE 3: Active site interactions in the CBL•4-CB-AMP structure. (A) Stereorepresentation of the active site of CBL bound to the adenylate structure. Protein atoms are shown in yellow (carbon), red (oxygen), and blue (nitrogen) in stick representation while the molecule of 4-CB-AMP is shown as ball-and-stick with gray carbon atoms, blue nitrogens, red oxygens, orange phosphorus atoms, and a green chlorine atom. Specific interactions discussed in the text are represented with dashed lines. Note that Lys492 is disordered beyond the Cβ atom. (B) The active site interactions are shown in a schematic representation. Interactions observed in the CBL structure are shown by black hashed lines.

bond between Asn302 and the N6 amino group of the adenine base. Tyr304 stacks against the adenine base. The ribose 2′ and 3′ hydroxyls interact with Asp385 and Arg400. The α-phosphate observed in the adenylate interacts with side chains Thr161 and Thr307. Thr161 is the first residue of the highly conserved motif 1 loop, while Thr307 is conserved within motif 2. His207 forms a hydrogen bond with the bridging oxygen between the 4-CB group and the AMP.

The 4-CBA-AMP adenine ring is sandwiched between the backbone of residues Gly281-Thr283 and the aromatic side chain of Tyr304. Other members of the family maintain an aromatic residue at this position with Tyr, Phe, or Trp more prominent in different subfamilies. Residues Gly281-Thr283 of the CBL(4-CB) complex (*18*) adopt a significantly different conformation compared to the homologous residues of Acs (Gly387-Pro389). In the structure of the CBL(4-CB-AMP) complex these three residues reorient to form a planar backbone that stacks against the adenine ring, similar to the orientation of this region in other family members (*9, 18*).

Together, these results identify interacting residues that are further explored with site-directed mutagenesis and kinetic analyses of the individual reactions in the accompanying manuscript (*30*).

Mg^{2+} and Phosphate Binding Regions. The current structure displays no electron density for the Mg^{2+} ion or the product PP_i. Of the previously reported structures of enzymes of the adenylate-forming family, only two (*17, 21*) contain a Mg^{2+} bound at the active site. In both structures, the metal ion is coordinated by one oxygen of the nucleotide α-phosphate and the side chains of the homologues of CBL residues Thr161 and Glu308. The lack of the metal ion in the CBL(4-CB-AMP) crystal structure allows the side chain of Thr161 to interact with the phosphate oxygen in place of the metal interaction (Figure 3B). A newly deposited structure of a human medium chain acyl-CoA synthetase bound to Mg•ATP yields important new insights into the ATP binding pocket (see Discussion).

Structure of CBL in the Thioester-forming Conformation. The CBL enzyme co-crystallized with AMP and 4-CP-CoA in the orthorhombic space group $P2_12_12_1$ with cell dimensions of $a = 60.5$ Å, $b = 87.8$ Å, and $c = 186.1$ Å. This new crystal form differed from all previously determined structures of CBL in the adenylate-forming conformation. To avoid any bias in the structure determination, only the N-terminal domain of wild-type CBL was used as a molecular replacement search model. The C-terminal domain was modeled into the observed density and the two subunits

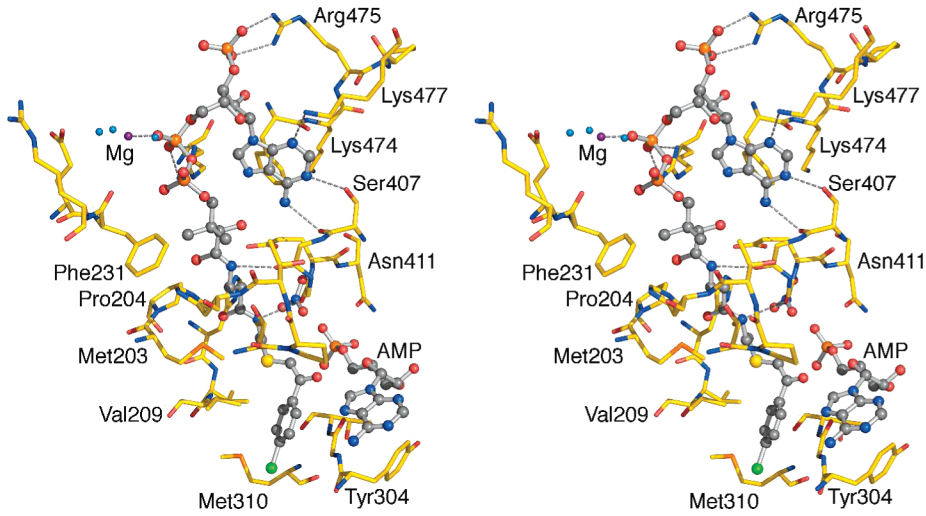

FIGURE 4: Active site interactions in the CBL•4-chlorophenacyl-CoA•AMP structure. The residues that form the CoA binding site are shown. All protein residues are shown using yellow sticks for carbon atoms, red for oxygen, blue for nitrogen, and orange for sulfurs. The ligands are shown in ball-and-stick format with gray carbon atoms, red oxygen atoms, blue nitrogen atoms, orange phosphorus atoms, yellow sulfur atoms, and green chlorine atoms. The Mg^{2+} cofactor is shown in purple with the coordinating waters shown in light blue. Dashed lines are shown for interactions between the protein and the ligands. Also shown near the phosphate of the AMP is a nitrate ion that was modeled into density in both subunits.

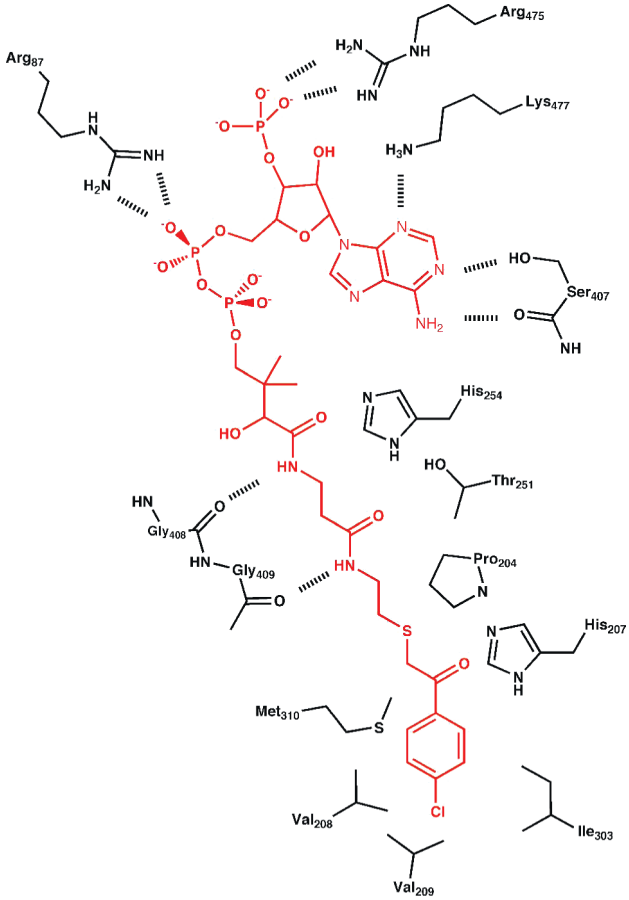

FIGURE 5: Schematic representation of the interactions between the protein residues (black) and the 4-chlorophenacyl-CoA inhibitor.

were then completed through iterative refinement and model building. The two molecules in the asymmetric unit superimpose very well, diverging only at the C-terminus where residues 485−503 adopt slightly different positions between the two subunits. All contacts made between the proteins and the ligands are conserved between the two subunits. The two molecules in the asymmetric unit are aligned along the same dimer interface as that seen along the crystallographic 2-fold in the trigonal space group for conformation 1. The homodimeric packing along the N-terminal domain of the CBL enzyme is thus consistent in the two crystal forms.

The overall appearance of the new CBL structure is very similar to that of structure of the prokaryotic Acs structure bound to adenosine-5′-propylphosphate and CoA. The 370 homologous Cα positions of Acs and CBL superimpose with an rms distance of 2.2 Å. Alignments of the individual domains yield an rms distance of 1.7 Å for the N-terminal domains (over 296 amino acids) or 1.3 Å for the C-terminal domain (over 75 residues). The N-terminal domain of the new CBL structure has an rms distance of less than 1 Å compared to the N-terminal domain of CBL in the adenylate-forming conformation. The N-terminal domain has not changed, except at residues that help stabilize the thioester-forming conformation. Residue Asp402, the hinge residue that bridges the N-terminal and C-terminal domain, showed significant torsional changes with phi and psi angles of −90° and −164° compared to −74° and −29° in the adenylate-forming conformation. These phi and psi angles for the thioester-forming conformation are very similar to prokaryotic Acs hinge residue Asp517 with phi and psi angles of −103° and −169°.

The AMP Binding Pocket of CBL in the Thioester-Forming Conformation. Unambiguous electron density was identified for both the 4-CP-CoA and AMP (Figure 2B). The AMP binds in the same location observed for the AMP moiety of the 4-CB-AMP ligand of CBL in the adenylate-forming conformation. The orientation of the adenine base is identical. The ribose moiety adopts a slightly different orientation in the second conformation, allowing both the 2′ and 3′ hydroxyls to interact with the side chain of Asp385, as observed in prior adenylate-forming enzymes. The AMP phosphate of the thioester-forming conformation is moved ∼1.7 Å from the phosphate in the adenylate complex likely reflecting the presence of the inhibitor in the active site. The rotation of the hinge residue Asp402 allows it to stabilize Arg400, which then interacts with the 3′-hydroxyl of AMP.

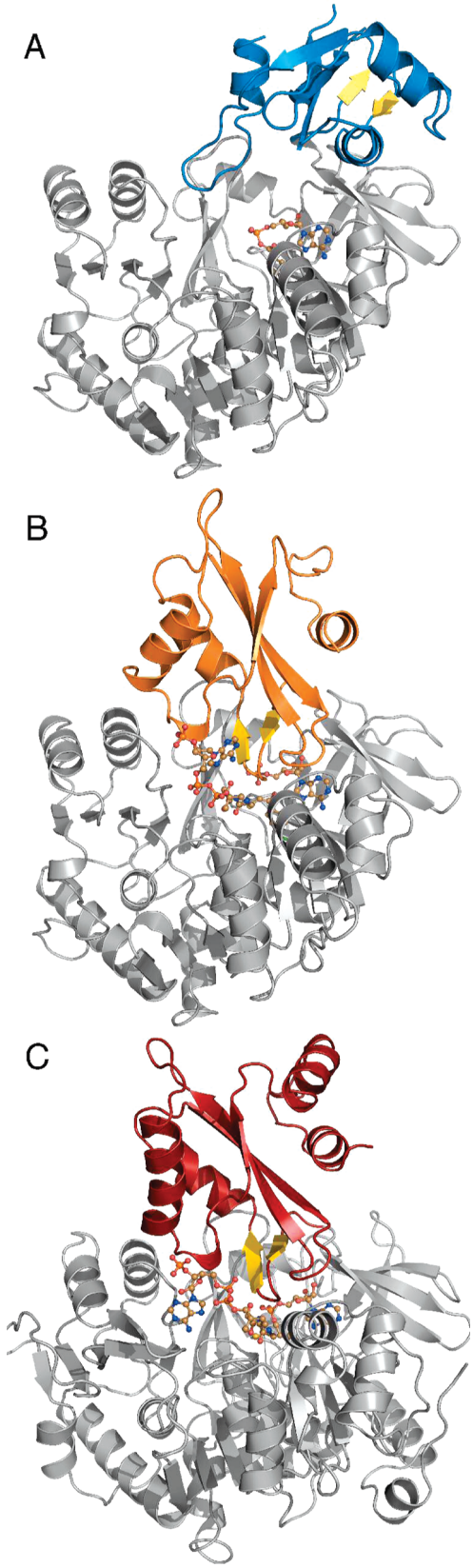

FIGURE 6: Three dimensional ribbon diagrams of (A) CBL bound to the adenylate, (B) CBL bound to 4-chlorophenacyl-CoA inhibitor and AMP, and (C) Acs bound to CoA and adenosine-5′-propylphosphate (1PG4). The N-terminal domains of all three proteins are colored gray, while the C-terminal domains are shown in blue, orange, and red. The A8 loop that follows the hinge residue (Asp402 in CBL and Asp517 in Acs) is colored with two yellow strands. Ligands are shown for all proteins, the 4-CB-AMP adenylate in panel A, 4-chlorophenacyl-CoA and AMP in panel B, and CoA and adenosine-5′-propylphosphate in panel C.

The Coenzyme A Binding Pocket of CBL. The CoA binding pocket (Figures 4 and 5) of the adenylate-forming enzymes can be divided into two components. The CoA nucleotide binds on the surface of the protein where it interacts with both the N- and C-terminal domains (Figure 6B). The phosphopantetheine group then passes through a tunnel that projects from the surface of the protein toward the buried active site. The pantetheine of the CBL inhibitor projects more deeply into the active site of CBL when compared to the CoA of Acs. In the Acs structure (*9*) the thiol of CoA is pushed away from the adenylate because of the alkyl-AMP ligand. Despite this difference, the pantetheine tunnel is similar between the two structures. The amide nitrogen from the β-alanine group of the pantetheine interacts with the carbonyl oxygen of Gly408, a residue on the A8 loop following the Asp402 hinge. This same interaction is observed in Acs. The amide nitrogen of the cysteamine group interacts with the carbonyl of Gly409 in CBL, an interaction that is 3.4 Å in Acs.

The comparison of the CBL and Acs structures illustrates that the pantetheine tunnel of the CBL is more constrained and may serve to better anchor the pantetheine group. In the Acs structures (*9, 10*), the nucleotide portion of CoA was very well ordered, whereas the density for the pantetheine was not of comparable quality. Several Ala residues in Acs (Ala305, Ala 354, and Ala357) are replaced in CBL with larger residues (Met203, Thr251, and His254, respectively) whose side chains constrict the pantetheine tunnel.

While these differences in the pantetheine tunnel are relatively minor, the nucleotide moiety of CoA binds in a significantly different conformation compared to the nucleotide of CoA bound to Acs. The base of CoA is rotated nearly 180° from the orientation observed in Acs (Figures 6 and 7). As a result, the CoA engages in many more interactions with the C-terminal domain in CBL than is observed in Acs. The CoA nucleotide-binding pocket in CBL is composed of residues Arg87, Ser407, G408, G409, Trp440, Phe473, Arg475, and Lys477. Of the residues that interact with the CoA nucleotide, the only N-terminal residue is Arg87, which interacts with the 5′ diphosphate of CoA. CoA bound to Acs interacts in the opposite fashion with seven of the eight residues that make up the CoA binding motif located on the N-terminal domain. Arg584 of Acs is the only residue located on the C-terminal domain that interacts with the 3′-phosphate of CoA. This accommodating binding pocket for the CoA base appears to be one consequence of the domain rotation in CBL.

DISCUSSION

There are currently nine adenylate-forming enzymes that have been characterized by X-ray crystallography. Of those nine, only three structures represent the thioester-forming conformation. The other six are either found in the adenylate-forming conformation or some intermediate conformation. CBL represents the only adenylate-forming enzyme solved in both the adenylate-forming conformation and thioester-forming conformation bound to ligands that represent the different states of the multistep reaction. Additionally, the CBL structure bound to AMP and 4-chlorophenacyl-CoA is the second enzyme bound with a thiol substrate and identifies a novel binding pocket for the CoA nucleotide that is located

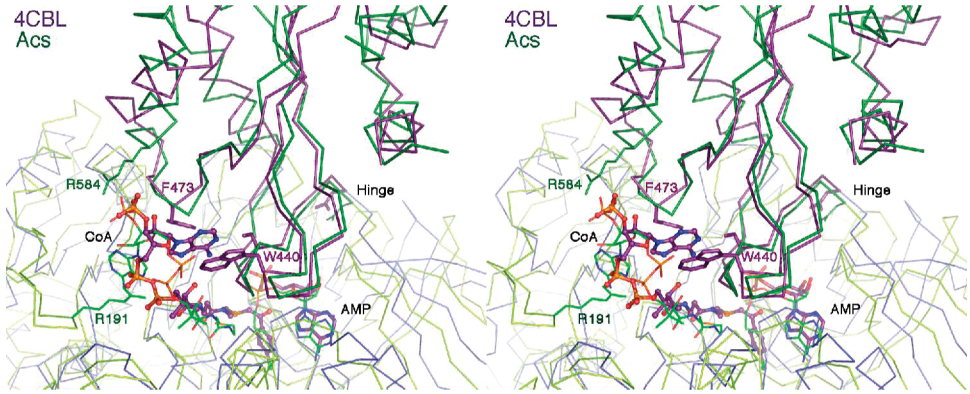

FIGURE 7: Comparison of the CoA binding pockets of CBL and Acs in the thioester-forming conformation. The CBL structure is shown in a Cα trace shown in blue for the N-terminal domain and purple for the C-terminal domain. Ligands from the CBL structure are shown with purple carbon atoms, red oxygens, blue nitrogens, orange phosphates, a yellow sulfur atom and a green chlorine atom. The side chains of Ser407, Trp440, and Phe473 are shown interacting with the nucleotide of CoA. The Acs structure was superimposed on CBL based on all homologous Cα positions. This structure is also shown as as a Cα trace with a light green N-terminal domain and a darker green C-terminal domain; the Acs structure includes the ligands CoA and adenosine-5′-propylphosphate. The side chains of Arg191 and Arg584 from Acs are shown. The Acs ligands and residue side chains are shown with thinner sticks than the CBL ligands; the Acs atoms are shown with the same color scheme as CBL except that carbons are colored green. The hinge residues Asp402 (CBL) and Asp517 (Acs) are also included.

on the C-terminal domain. These structures support and shed new light on the domain alternation theory of catalysis by the adenylate-forming enzymes.

The opposite faces of the C-terminal domain interact with the active site in the two conformations (Figure 6A,B). Two residues best illustrate the magnitude of the effect of the domain movement. The universally conserved Lys492 of the A10 region that is located at the active site in the adenylate-forming conformation is now 21.5 Å away from that position and is directed into solvent in the thioester-forming conformation. Conversely, Gly408 which is completely conserved within the A8 region, is 32.0 Å from its position in the first half-reaction. In the thioester-forming conformation, Gly408 is positioned at the active site where it hydrogen bonds to the phosphopantetheine moiety of CoA.

Several new interactions are observed between residues in the N-terminal domain that appear to stabilize the thioester-forming conformation. As described above, the conserved A3 region (residues 161−169) that is rich in glycine and serine/threonine is thought to play a key role in the orientation of the phosphates of ATP. This loop also interacts with the C-terminal domain in the thioester-forming conformation as the main chain carbonyl of Thr164 interacts with His413 to stabilize this conformation.

Until recently, no structures of members of the adenylate-forming family have been determined with ATP in the active site. The structure of the long-chain acyl-CoA synthetase (*21*) was determined with AMPPNP bound in the active site. This structure, however, does not contain an acyl ligand and the β and γ phosphates are not properly oriented for in-line attack of the acyl substrate from the acyl binding pocket toward the α phosphate to displace the PP_i leaving group. Two structures have recently been determined by the Structural Genomics Consortium in Toronto (unpublished, PDB accession codes 3B7W and 3C5E) of a human medium chain acyl-CoA synthetase. These structures illustrate the two observed conformations for members of the adenylate-forming family. In the unliganded form, the enzyme adopts the thioester-forming conformation while a structure bound to Mg•ATP and an unknown acyl ligand crystallized in the adenylate-forming conformation. This structure provides the exciting first glimpse of the binding interaction of Mg•ATP within this enzyme family. In the 3C5E structure, the Mg^{2+} is coordinated to two oxygens from the β- and γ-phosphates of ATP and to four water molecules. Two of the waters interact with the homologue of CBL Glu308.

His207 adopts a different side chain conformation in the two structures of CBL. In the adenylate-forming conformation, His207 is oriented 3.0 Å from the carboxyl oxygen of 4-CB. In the thioester-forming conformation, Glu410 from the C-terminal domain is rotated into the active site and interacts with the side chain of His207. This interaction pulls His207 out of the active site to free the space occupied by the thiol of CoA as it approaches the active site. As described in the accompanying manuscript, mutation of His207 has a signficant effect on the microscopic rate constants for the two half-reactions. His207 therefore plays a catalytic role by aligning the carboxylate for the adenylation half-reaction and then plays a substantial role in stabilizing the CBL protein in the thioester-forming conformation.

The new CBL structure identifies a novel CoA binding pocket that is distinct compared to the CoA binding pocket of Acs (Figure 7). Instead of interacting primarily with the N-terminal domain as observed in the Acs structure (*9*), the adenine ring of CoA binds in a groove in the C-terminal domain in CBL. Arginine residues engage in ion pair formation with the phosphates of CoA in both Acs and CBL structures. There are two arginines that interact with CoA in CBL. Arg87 interacts with the 5′-diphosphate of CoA, and in the Acs structure a glycine (Gly165) occupies this location. Arg475 located on the C-terminal domain interacts with the 3′-phosphate of CoA. Arg584 of Acs is similarly located and it has been shown to play a key role in CoA binding (*10*).

The phosphopantetheine moiety of CoA must traverse through a tunnel composed of residues located on both the N- and C-terminal domains and ends in the vicinity of the AMP and substrate binding pockets (Figures 4 and 5). The majority of residues that make up this tunnel are located on the N-terminal domain. The C-terminal domain residues that

form this tunnel are located in the A8 region and contain a highly conserved glycine (Gly409 in CBL). The conserved glycine in the A8 region was mutated to a leucine in Acs and kinetic analysis showed the mutant to be only active for the adenylate-forming half-reaction (*10*). Mutation of this glycine to alanine in CBL (*30*) results in a decrease in catalytic efficiency for CoA by 3 orders of magnitude emphasizing the more constrained pantetheine binding tunnel of CBL compared to Acs. Gly281 of CBL, a residue that stacks against the adenine base of ATP as discussed earlier, also abuts the pantetheine tunnel near the acyl-binding pocket. This glycine residue is most likely conserved to allow the phosphopantetheine tunnel to remain open; a substitution of a larger residue would disrupt the thioester-forming half-reaction.

As our original structure of Acs bound to CoA represented the only enzyme crystallized in the thioester-forming conformation (*9*), we originally proposed that it was the binding of CoA that triggered the conformational change. This hypothesis is supported by the new structure of CBL; however, the human acyl-CoA synthetase described above (3B7W) demonstrates that in the absence of ligands the enzyme adopts the thioester-forming conformation.

We considered the possibility that crystal contacts are stabilizing the observed conformations. Interactions are indeed made between the C-terminal domains of both conformations of CBL in their respective crystal forms. We computationally analyzed whether placement of either conformation of CBL into the "wrong" crystal form, that is, putting conformation 1 into the orthorhombic crystal form or conformation 2 into the trigonal form-creates steric clashes between symmetry-related protein molecules. The trigonal form where we observed conformation 1 is indeed able to accommodate either conformation, while the orthorhombic form cannot accommodate the adenylate-forming conformation. We believe however that the observed conformations are driven primarily by the ligands present. It is then the protein conformation that dictates crystallization and not crystallization conditions that lead to a specific protein conformation. In support of this, we have been unable to crystallize CBL or Acs in alternate conformations in the absence of the proper ligands. More importantly, the two conformations of CBL superimpose very closely to the conformations observed for other family members, most notably Acs which has been crystallized in the adenylate-forming conformation for the yeast isozyme (*22*) and the thioester-forming conformation for the bacterial enzyme (*9*).

We now propose that there is an equilibrium between these two conformational states, and our earlier predictions that CoA binding is sufficient to drive the change to the thioester-forming conformation were overly simplified. It is likely that in the absence of ligands, this conformational equilibrium differs for different proteins within the family, and each member may have a preferred state where the protein is more likely to crystallize. Binding of ligands will induce the protein into one of these two conformations because of the steric interactions in the wrong conformation. The thioester-forming conformation cannot bind to ATP, because of the interaction between the A8 loop and the β,γ-phosphates. Similarly, conformation 1 cannot bind CoA because of the interaction of the pantetheine group and His207.

All of our structural and biochemical results with Acs and CBL are consistent with independent catalysis of the two half-reactions using the two observed conformations. The kinetic data presented in the accompanying paper in this issue also support this hypothesis as residues on opposite faces of the C-terminal domain selectively affect one of the two half-reactions. The two half-reactions are catalyzed in a ping-pong mechanism, in which the kinetically independent steps are separated by the domain rotation. The numerous contacts made between CoA and the C-terminal domain in CBL, combined with the kinetic analysis, allow us to propose a plausible explanation for the use of domain alternation by the adenylate-forming enzymes (*30*) in which the role of the domain movement is to remove stabilizing residues that are necessary for the adenylation half-reaction from the active site and simultaneously create a binding pocket for the CoA nucleotide.

ACKNOWLEDGMENT

We thank Joe Luft and Jennifer Wolfley for assistance with crystallization screening and optimization and Dr. Edward Snell for assistance with the remote synchrotron data collection.

REFERENCES

1. Amyes, T. L., and Richard, J. P. (2007) Enzymatic catalysis of proton transfer at carbon: activation of triosephosphate isomerase by phosphite dianion. *Biochemistry 46*, 5841–5854.
2. Bertrand, J. A., Auger, G., Martin, L., Fanchon, E., Blanot, D., Le.Beller, D., van.Heijenoort, J., and Dideberg, O. (1999) Determination of the MurD mechanism through crystallographic analysis of enzyme complexes. *J. Mol. Biol. 289*, 579–590.
3. Leys, D., Tsapin, A. S., Nealson, K. H., Meyer, T. E., Cusanovich, M. A., and Van Beeumen, J. J. (1999) Structure and mechanism of the flavocytochrome c fumarate reductase of Shewanella putrefaciens MR-1. *Nat. Struct. Biol. 6*, 1113–1117.
4. Jenni, S., Leibundgut, M., Maier, T., and Ban, N. (2006) Architecture of a fungal fatty acid synthase at 5 Å resolution. *Science 311*, 1263–1267.
5. Leibundgut, M., Jenni, S., Frick, C., and Ban, N. (2007) Structural basis for substrate delivery by acyl carrier protein in the yeast fatty acid synthase. *Science 316*, 288–290.
6. St Maurice, M., Reinhardt, L., Surinya, K. H., Attwood, P. V., Wallace, J. C., Cleland, W. W., and Rayment, I. (2007) Domain architecture of pyruvate carboxylase, a biotin-dependent multifunctional enzyme. *Science 317*, 1076–1079.
7. Lim, K., Read, R. J., Chen, C. C., Tempczyk, A., Wei, M., Ye, D., Wu, C., Dunaway-Mariano, D., and Herzberg, O. (2007) Swiveling domain mechanism in pyruvate phosphate dikinase. *Biochemistry 46*, 14845–14853.
8. Bandarian, V., Pattridge, K. A., Lennon, B. W., Huddler, D. P., Matthews, R. G., and Ludwig, M. L. (2002) Domain alternation switches B(12)-dependent methionine synthase to the activation conformation. *Nat. Struct. Biol. 9*, 53–56.
9. Gulick, A. M., Starai, V. J., Horswill, A. R., Homick, K. M., and Escalante-Semerena, J. C. (2003) The 1.75 Å crystal structure of acetyl-CoA synthetase bound to adenosine-5′-propylphosphate and coenzyme A. *Biochemistry 42*, 2866–2873.
10. Reger, A. S., Carney, J. M., and Gulick, A. M. (2007) Biochemical and crystallographic analysis of substrate binding and conformational changes in acetyl-CoA synthetase. *Biochemistry 46*, 6536–6546.
11. Babbitt, P. C., Kenyon, G. L., Martin, B. M., Charest, H., Slyvestre, M., Scholten, J. D., Chang, K. H., Liang, P. H., and Dunaway-Mariano, D. (1992) Ancestry of the 4-chlorobenzoate dehalogenase: analysis of amino acid sequence identities among families of acyl: adenyl ligases, enoyl-CoA hydratases/isomerases, and acyl-CoA thioesterases. *Biochemistry 31*, 5594–5604.
12. Scholten, J. D., Chang, K. H., Babbitt, P. C., Charest, H., Sylvestre, M., and Dunaway-Mariano, D. (1991) Novel enzymic hydrolytic dehalogenation of a chlorinated aromatic. *Science 253*, 182–185.

13. Turgay, K., Krause, M., and Marahiel, M. A. (1992) Four homologous domains in the primary structure of GrsB are related to domains in a superfamily of adenylate-forming enzymes. *Mol. Microbiol. 6*, 529–546.
14. Chang, K. H., Xiang, H., and Dunaway-Mariano, D. (1997) Acyl-adenylate motif of the acyl-adenylate/thioester-forming enzyme superfamily: a site-directed mutagenesis study with the Pseudomonas sp. strain CBS3 4-chlorobenzoate:coenzyme A ligase. *Biochemistry 36*, 15650–15659.
15. Marahiel, M. A., Stachelhaus, T., and Mootz, H. D. (1997) Modular peptide synthetases involved in nonribosomal peptide synthesis. *Chem. Rev. 97*, 2651–2674.
16. Conti, E., Franks, N. P., and Brick, P. (1996) Crystal structure of firefly luciferase throws light on a superfamily of adenylate-forming enzymes. *Structure 4*, 287–298.
17. Conti, E., Stachelhaus, T., Marahiel, M. A., and Brick, P. (1997) Structural basis for the activation of phenylalanine in the nonribosomal biosynthesis of gramicidin S. *EMBO J. 16*, 4174–4183.
18. Gulick, A. M., Lu, X., and Dunaway.Mariano, D. (2004) Crystal structure of 4-chlorobenzoate:CoA ligase/synthetase in the unliganded and aryl substrate-bound states. *Biochemistry 43*, 8670–8679.
19. Wu, R., Reger, A. S., Cao, J., Gulick, A. M., and Dunaway-Mariano, D. (2007) Rational redesign of the 4-chlorobenzoate binding site of 4-chlorobenzoate: coenzyme a ligase for expanded substrate range. *Biochemistry 46*, 14487–14499.
20. Bains, J., and Boulanger, M. J. (2007) Biochemical and structural characterization of the paralogous benzoate CoA ligases from Burkholderia xenovorans LB400: defining the entry point into the novel benzoate oxidation (box) pathway. *J. Mol. Biol. 373*, 965–977.
21. Hisanaga, Y., Ago, H., Nakagawa, N., Hamada, K., Ida, K., Yamamoto, M., Hori, T., Arii, Y., Sugahara, M., Kuramitsu, S., Yokoyama, S., and Miyano, M. (2004) Structural basis of the substrate-specific two-step catalysis of long chain fatty acyl-CoA synthetase dimer. *J. Biol. Chem. 279*, 31717–31726.
22. Jogl, G., and Tong, L. (2004) Crystal structure of yeast acetyl-coenzyme A synthetase in complex with AMP. *Biochemistry 43*, 1425–1431.
23. May, J. J., Kessler, N., Marahiel, M. A., and Stubbs, M. T. (2002) Crystal structure of DhbE, an archetype for aryl acid activating domains of modular nonribosomal peptide synthetases. *Proc. Natl. Acad. Sci. U. S. A. 99*, 12120–12125.
24. Nakatsu, T., Ichiyama, S., Hiratake, J., Saldanha, A., Kobashi, N., Sakata, K., and Kato, H. (2006) Structural basis for the spectral difference in luciferase bioluminescence. *Nature 440*, 372–376.
25. Stachelhaus, T., Mootz, H. D., and Marahiel, M. A. (1999) The specificity-conferring code of adenylation domains in nonribosomal peptide synthetases. *Chem. Biol. 6*, 493–505.
26. Ingram-Smith, C., Woods, B. I., and Smith, K. S. (2006) Characterization of the acyl substrate binding pocket of acetyl-CoA synthetase. *Biochemistry 45*, 11482–11490.
27. Eppelmann, K., Stachelhaus, T., and Marahiel, M. A. (2002) Exploitation of the selectivity-conferring code of nonribosomal peptide synthetases for the rational design of novel peptide antibiotics. *Biochemistry 41*, 9718–9726.
28. Branchini, B. R., Southworth, T. L., Murtiashaw, M. H., Wilkinson, S. R., Khattak, N. F., Rosenberg, J. C., and Zimmer, M. (2005) Mutagenesis evidence that the partial reactions of firefly bioluminescence are catalyzed by different conformations of the luciferase C-terminal domain. *Biochemistry 44*, 1385–1393.
29. Chang, K. H., Liang, P. H., Beck, W., Scholten, J. D., and Dunaway-Mariano, D. (1992) Isolation and characterization of the three polypeptide components of 4-chlorobenzoate dehalogenase from Pseudomonas sp. strain CBS-3. *Biochemistry 31*, 5605–5610.
30. Wu, R., Cao, J., Lu, X., Reger, A. S., Gulick, A. M., and Dunaway-Mariano, D. (2008) Mechanism of 4-chlorobenzoate: coenzyme A ligase catalysis. *Biochemistry 47*, 8026–8039.
31. Gulick, A. M., Horswill, A. R., Thoden, J. B., Escalante-Semerena, J. C., and Rayment, I. (2002) Pentaerythritol propoxylate: a new crystallization agent and cryoprotectant induces crystal growth of 2-methylcitrate dehydratase. *Acta Crystallogr. D58*, 306–309.
32. Vagin, A., and Teplyakov, A. (1997) MOLREP: an automated program for molecular replacement. *J. Appl. Crystallogr. 30*, 1022–1025.
33. CCP4. (1994) The CCP4 suite: programs for protein crystallography. *Acta Crystallogr. D50*, 760−763.
34. Murshudov, G. N., Vagin, A. A., and Dodson, E. J. (1997) Refinement of macromolecular structures by the maximum-likelihood method. *Acta Crystallogr. D53*, 240–255.
35. Winn, M. D., Isupov, M. N., and Murshudov, G. N. (2001) Use of TLS parameters to model anisotropic displacements in macromolecular refinement. *Acta Crystallogr. D57*, 122–133.
36. Luo, L., Taylor, K. L., Xiang, H., Wei, Y., Zhang, W., and Dunaway-Mariano, D. (2001) Role of active site binding interactions in 4-chlorobenzoyl-coenzyme A dehalogenase catalysis. *Biochemistry 40*, 15684–15692.
37. Luft, J. R., Collins, R. J., Fehrman, N. A., Lauricella, A. M., Veatch, C. K., and DeTitta, G. T. (2003) A deliberate approach to screening for initial crystallization conditions of biological macromolecules. *J. Struct. Biol. 142*, 170–179.
38. Luft, J. R., Wolfley, J. R., Said, M. I., Nagel, R. M., Lauricella, A. M., Smith, J. L., Thayer, M. H., Veatch, C. K., Snell, E. H., Malkowski, M. G., and Detitta, G. T. (2007) Efficient optimization of crystallization conditions by manipulation of drop volume ratio and temperature. *Protein Sci. 16*, 715–722.
39. Rayment, I. (2002) Small-scale batch crystallization of proteins revisited: an underutilized way to grow large protein crystals. *Structure 10*, 147–151.
40. McPhillips, T. M., McPhillips, S. E., Chiu, H. J., Cohen, A. E., Deacon, A. M., Ellis, P. J., Garman, E., Gonzalez, A., Sauter, N. K., Phizackerley, R. P., Soltis, S. M., and Kuhn, P. (2002) Blu-Ice and the Distributed Control System: software for data acquisition and instrument control at macromolecular crystallography beamlines. *J. Synchrotron Radiat. 9*, 401–406.
41. Kabsch, W. (1988) Evaluation of single-crystal X-ray diffraction data from a position-sensitive detector. *J. Appl. Crystallogr. 21*, 916–924.
42. Emsley, P., and Cowtan, K. (2004) Coot: model-building tools for molecular graphics. *Acta Crystallogr. D60*, 2126–2132.
43. Hayward, S., and Lee, R. A. (2002) Improvements in the analysis of domain motions in proteins from conformational change: DynDom version 1.50. *J. Mol. Graphics Modelling 21*, 181–183.
44. DeLano, W. L. (2002) The PYMOL Molecular Graphics System, http://www.pymol.org.

BI800696Y